Int. J. Electrochem. Sci., 8 **(2013)** 4571 - 4582

International Journal of
ELECTROCHEMICAL
SCIENCE
www.electrochemsci.org

Corrosion of Nickel-Aluminum-Bronze Alloy in Aerated 0.1 M Sodium Chloride Solutions under Hydrodynamic Condition

Abdul Amir H. Kadhum[1], *Abu Bakar Mohamad*[1], *Huda Dhia Jaffar*[2] , *Sam Sin Yan*[1], *Jasim Hilo Naama*[3], *Ali A Al-Tamimi*[3], *Redah I. Al-Bayati*[3], *Ahmed A. Al-Amiery*[1,3,*]

[1] Department of Chemical and Process Engineering, Faculty of Engineering and Built Environment, Universiti Kebangsaan Malaysia, Bangi, Selangor 43600, Malaysia;
[2] College of Education, Baghdad University, Baghdad, Iraq
[3] Biotechnology Division, Applied Science Department, University of Technology, Baghdad 10066, Iraq
[*]E-mail: dr.ahmed@eng.ukm.my; dr.ahmed1975@gmail.com

Received: 21 November 2012 / *Accepted:* 5 March 2013 / *Published:* 1 April 2013

The issue of corrosion is a major problem on equipments failure and damage in industrial that would affect the safety and efficiency of the equipments. This study is focused on the corrosion of Nickel-Aluminiu-Bronze (NAB) alloy in aerated 0.1 M sodium chloride solution under hydrodynamic condition at 30^{o}C. Hydrodynamic conditions are simulated by using rotating cylinder electrode (RCE) with five sets rotational speed which are 400, 800, 1200, 1600 and 2000 rpm. Electrochemical measurements such as open circuit potential, electrochemical impedance spectroscopy and potentiodynamic were used to study the corrosion mechanism and corrosion rate of NAB alloy. Results revealed that the formation of oxide layer and the corrosion rate were influenced by rotational speed. The value of open circuit potential is found to be shifted to more negative direction, the corrosion current density is increased while the charge transfer resistance decreased with rotational speed.

Keywords: Nickel-Aluminiu-Bronze alloy, corrosion, potentiodynamic, Tafel

1. INTRODUCTION

The Aluminium-Bronze alloys are a family of copper-base alloys containing approximately 5% to 11% aluminium, some having additions of iron, nickel, manganese or silicon. They include alloys suitable for sand casting, gravity diecasting and for the production of forgings, plate, sheet, tube, strip, wire and extruded rods and sections. Compared with other copper alloys, the higher strength of the aluminium bronzes is combined with excellent corrosion resistance under a wide range of service

conditions. Nickel–Aluminum Bronze (NAB) alloys offer high strength, high corrosion resistance and are available in a number of different forms. Steady state corrosion rates for NAB alloys are in the order of 0.025 mmy in seawater conditions [1]. Aluminium bronzes are the most tarnish-resistant copper alloys and show no serious deterioration in appearance and no significant loss of mechanical properties on exposure to most atmospheric conditions [2-5]. Their resistance to atmospheric corrosion combined with high strength is exploited, for example, in their use for bearing bushes in aircraft frames [6-13]. Aluminium bronzes also show low rates of oxidation at high temperatures and excellent resistance to sulphuric acid, sulphur dioxide and other combustion products and are, therefore, used for the construction of items exposed to either or both these conditions. For example, aluminium bronzes are used very successfully for inert gas fans in oil tankers [14-19]. These operate under highly stressed conditions in a variable but very corrosive atmosphere containing salt-laden water vapour, sulphurous gases and carbon. The microstructure of the alloy consists of a Cu-rich solid solution known as α-phase and β′-phase or martensitic β-phase, surrounded by lamellar eutectoid phase and a series of intermatallic k phases [20,21]. No engineering alloy is immune to corrosion. Corrosion resistance depends upon the formation of a thin protective film or layer of corrosion products which prevents or substantially slows down the rate of attack. The aluminium content of aluminium bronzes imparts the ability to form, very rapidly, an alumina-rich protective film which is highly protective and is not susceptible to localised breakdown and consequent pitting in the presence of chlorides. Aluminium bronzes are, therefore, very resistant to corrosion by sea water and probably find more use in sea water service than in any other environment. Virtually all metals and alloys in common use are susceptible to some extent to crevice corrosion, i.e. accelerated attack within or just at the edge of areas shielded by close proximity to other components or by deposits on the surface.

The aim of this study is to investigate the corrosion behavior of the NAB alloy in simulated seawater under flow condition using open circuit potential (OCP), electrochemical impedance spectroscopy (EIS) and potentiodynamic polarization.

2. EXPEREMENTALS

2.1. Metal samples

Metal samples used in the study is that NAB alloy cylindrical shape with a diameter of 1.2 cm and a height value 0.78 cm and the active surface area of 2.94 cm^2 to fit into a rotating cylinder electrode.

Through testing of X-ray fluorescence (XRF) found that the chemical composition of the NAB alloy is 10 wt% Cl, 1.0 wt% Mn, 3.14 wt% Fe, 5:02 wt% Ni, 80.1 wt% Cu, 0.1 wt% Sr and 0.4wt% Yb.

The standard method ASTM G1-03 [22] for prepare, purify, and assess the corrosion tests on metal samples followed by providing a metal sample for testing, corrosion products after testing and evaluating the corrosion damage that has occurred.

2.2. Electrochemical measurement

All measurements were performed in triplicate, and average values are reported. Electrochemical measurements of steady state open circuit potentials (OCP) were conducted with Gamry water-jacketed glass cell. The cell contained three electrodes, the working, counter and reference electrodes, comprised of NAB alloy, a graphite bar and a calomel electrode (SCE), respectively. Measurements were performed using a Gamry Instrument Potentiostat/Galvanostat/ZRA model Ref 600. DC105 and EIS300 softwares by Gamry were used for potentiodynamic scans and electrochemical impedance spectroscopy (EIS). The potentiodynamic current-potential curves were swept from -0.25 to +0.25 V_{SCE} at a scan rate of 0.5 mVs^{-1}. Impedance measurements were carried out using AC signals of 5mV peak to peak amplitude at the open circuit potential in the frequency range 100 kHz–0.1 Hz. All impedance date were fitted to appropriate equivalent circuits (EC) using Gamry Echem Analyst software. Experiments for electrochemical measurements were initiated about 30 min after the working electrode was immersed in the solution to stabilize the steady state potential. The experiment started with the preparation of samples and the preparation of metal NAB alloy 0.1 M solution of sodium chloride and inflation for 20 minutes so that the solution becomes saturated. The solution temperature was maintained at $30^{o}C$ while rotating cylinder electrode rotation speed of 400 rpm pix, 800 rpm, 1200 rpm, 1600 rpm and 2000 rpm.

3. RESULTS AND DISCUSSION

3.1. Open circuit potential (OCP)

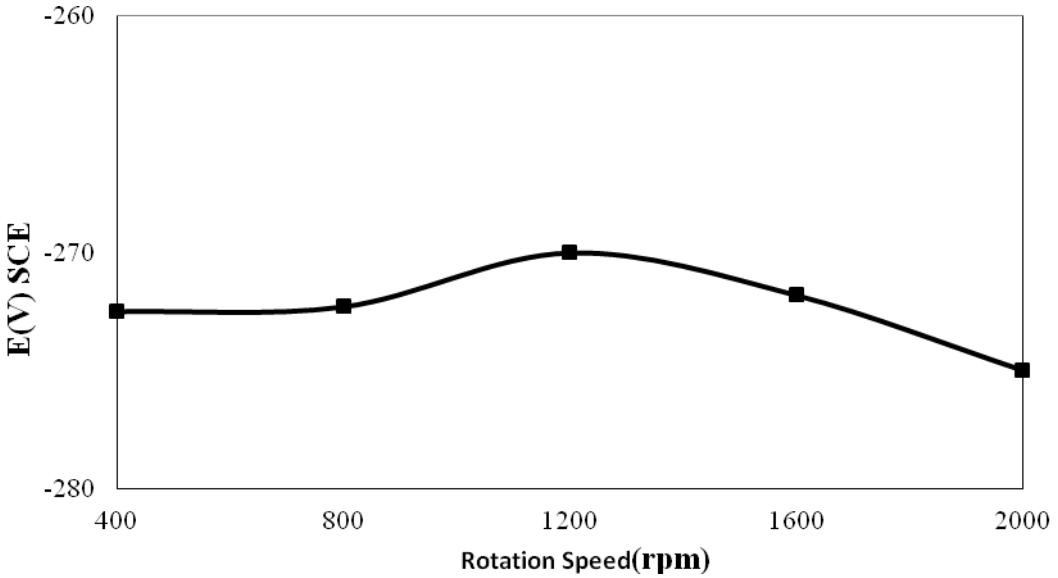

Figure 1. Changes in the value of the open circuit potential at different electrode rotation speed

NAB alloys are copper based alloys most resistant to the flow which causes corrosion. However, when the NAB alloy in aerated 0.1 M NaCl solution under hydrodynamic conditions at high speed or high turbulence levels, damage can occur to the protective oxide layer and the exposed metal [23-25]. Corrosion rate increases with flow as the dissolved oxygen began to come into contact with the metal. Metals generally have existing corrosion resistance there while the protective layer is formed on the metal surface of the corrosion process.

Open circuit potential is a parameter which indicates the tendency thermodynamic oxidative electrochemical materials in corrosive medium. OCP for NAB alloy was monitored over 60 minutes once soaked in aerated 0.1 M NaCl solution at 30 ^{o}C. This potential may vary with time due to changes in the nature of the electrode surface such as the formation of oxidation, the passive or immunity.

Figure 1 shows the behavior of NAB alloy immersed in aerated 0.1 M NaCl solution at a temperature of 30^{o}C with an electrode rotation speed of 400 rpm to 2000 rpm. According to Figure 1, the values of the open circuit potential of the NAB alloy shifted to a more negative potential with increasing rotational speed of the electrode reflects instability of the oxide layer on the alloy surface. This decline seems to be related to the formation and thinning of the oxide layer on the lower surface of the NAB alloy corrosion protection ability. With increased speed electrode, protective oxide layer on the alloy is not stable NAB and it is soluble in a solution of fast flowing.

Relatively, little work has been directed to study the electrochemical behavior of Cu–Al. A study of pure Cu and the three tested Cu alloys in the as-prepared 1 M NaCl solution (pH 6.5) for time duration of 1 h. The EOCP curves for Cu and Cu–Ni decreased upon specimen immersion before reaching the steady state value. A sharp decrease in EOCP was initially evident in the case of Cu–Al followed by an increase in EOCP to a value similar to that for pure Cu. [26].

3.2. Electrochemical impedance spectroscopy (EIS)

Electrochemical methods based on alternating currents can be used to obtain insights into corrosion mechanisms and to establish the effectiveness of corrosion control methods, such as inhibition and coatings. In an alternating - current circuit, impedance determines the amplitude of current for a given voltage. Impedance is the proportionality factor between voltage and current. In electrochemical impedance spectroscopy (EIS), the response of an electrode to alternating potential signals of varying frequency is interpreted on the basis of circuit models of the electrode/electrolyte interface [27].

Impedance measurements provide information on both the resistive and capacitive behavior of the interface, evaluation on the performance of studied compounds as possible corrosion inhibitor, and investigation of the corrosion inhibition processes.

EIS spectrum of the raw data at NAB alloy electrode for five different electrode rotation speed in aerated 0.1 M NaCl solution at a temperature of 30^{o}C was recorded in the form of Nyquist plots in Figure 2 to determine the influence of turbulent flow effects on corrosion behavior of NAB alloy. In addition, Figure 3 shows the Nyquist plots of the raw data adjustment using Gamry software analysis Echem through adaptive simplex method to obtain a more complete EIS spectrum. Referring to Figure

3, the Nyquist plot consists of semi-circular shaped capacitive loop related to charge transfer processes that occur during the dissolution and breakdown of the oxide layer on the alloy surface NAV. Nyquist plot showing corrosion resistance decreases with increasing rotational speed NAB alloy electrodes. The highest corrosion resistance $7.77\times10^{2}\ \Omega\ cm^{2}$ is the rotational speed of 400 rpm.

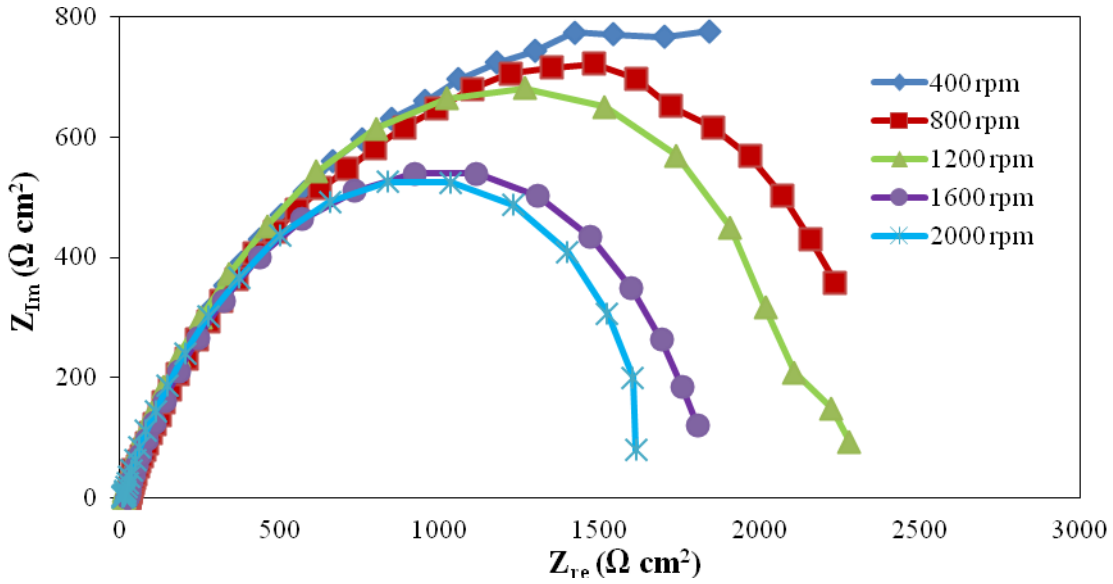

Figure 2. Nyquist plot of the for NAB alloy in 0.1 M aerated NaCl at 30 ^{o}C with different rotational speeds

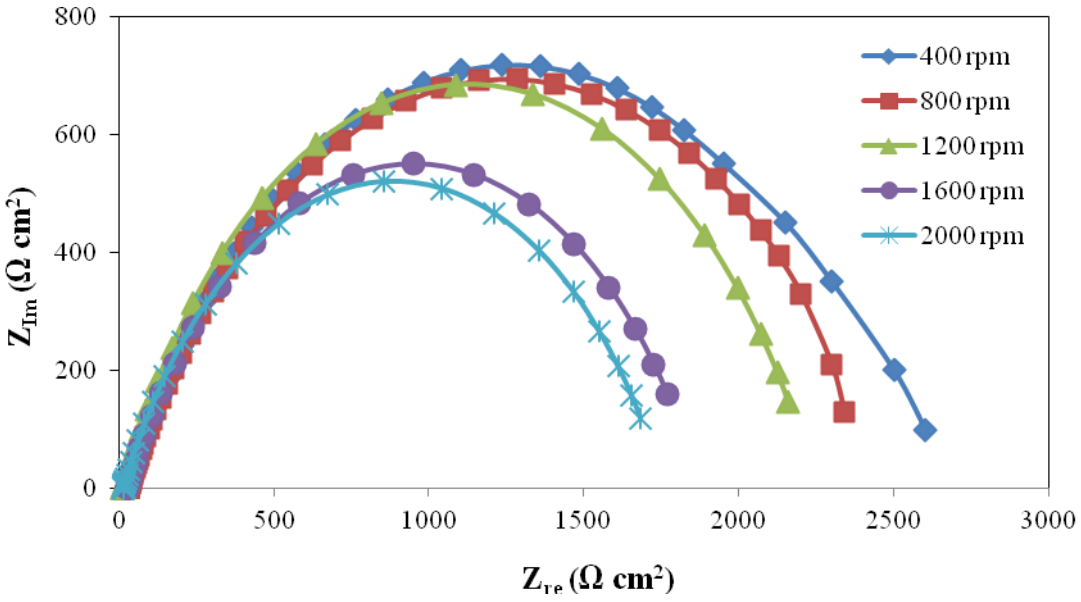

Figure 3. Nyquist plot of the simplex method using the analysis of adaptation Echem Gamry software for NAB alloys in aerated 0.1 M NaCl solution at 30^{o}C with different rotational speeds.

Similar results have been reported in the literature for the corrosion of aluminum [28-30].

Figure 4 shows the equivalent circuit model used to fit the impedance data for NAB alloys in aerated 0.1 M NaCl solution at a temperature of 30°C which consist of solution resistance (Rs) series with the charge transfer resistance (R_{ct}) then in parallel with the same phase element (CPE). Impedance and phase data in the form of Bode plots are illustrated in Figure 5 for the rotational speed of 400 rpm NAB alloy electrode in aerated 0.1 M NaCl solution at 30°C and shows the line fit (fitted line) using the circuit in Figure 4.

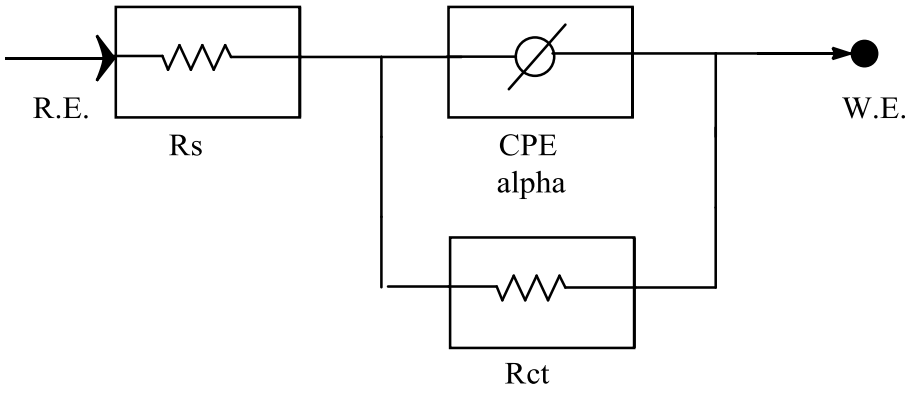

Figure 4. The equivalent circuit model used to fit the impedance data for NAB alloys in aerated 0.1 M NaCl solution at a temperature of 30 °C

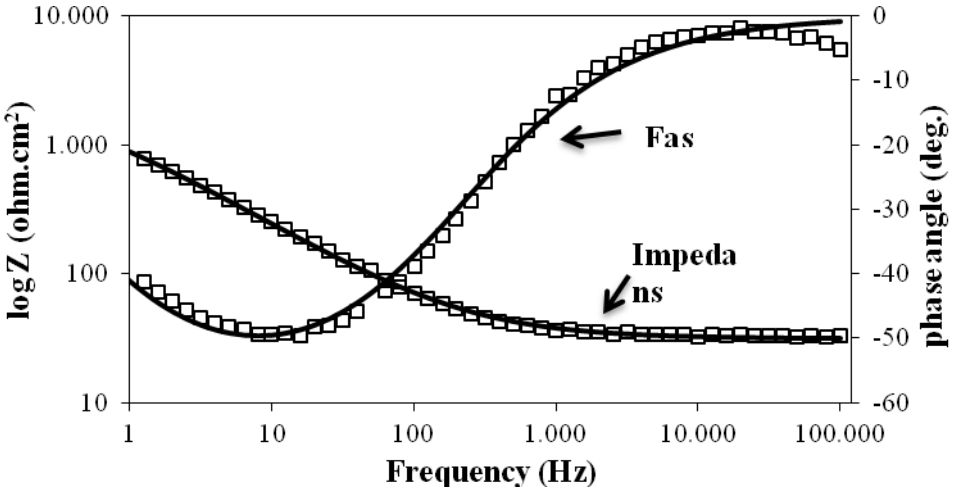

Figure 5. Bode plot of impedance and phase data for the rotational speed of 400 rpm NAB alloys in aerated 0.1 M NaCl solution at 30°C and shows the line fit (-) using the circuit in Figure 4.

Parameter values from EIS measurements were collected and tabulated in Table 1, including the charge transfer resistance, R_{ct}, solution resistance, R_s, same phase element, CPE, alpha, α and double layer capacitance, CDL. CDL value can be obtained through the following equation,

$$C_{dl} = (y_o \; R_{ct}^{\;1-\alpha})^{1/\alpha}$$

(1)

From EIS data found that RCT was decreased with increasing the rotational speed of the electrode alloy NAV. This shows that the corrosion rate will increase with high flow velocity the charge transfer resistance decreases.

Table 1. Data EIS for NAB alloys in aerated 0.1 M NaCl solution at a temperature 30 ^{o}C with different electrode rotational speed

Rotation Speed (rpm)	R_{ct} (kohms cm^2)	R_u (ohms cm^2)	CPE (Y_o) (x10^{-6}) (Ss^a/cm^2)	Alpha (α)	C_{dl} (mF/cm^2)
400	2.479	31.44	266.4	0.6680	216.76
800	2.433	30.29	454.3	0.6594	478.41
1200	2.232	12.90	248.4	0.6997	192.85
1600	1.847	27.38	394.5	0.6831	340.62
2000	1.782	13.89	326.3	0.6813	253.20

3.3. Polarization Potentiodynamic

Polarization curves obtained from various rotational speeds NAB alloy electrode in aerated 0.1 M NaCl solution at a temperature of 30^{o}C is shown in Figure 6. In addition, Figure 7 shows the polarization curve of adaptation Tafel method using Echem Gamry software analysis to obtain more perfect curves and clear.

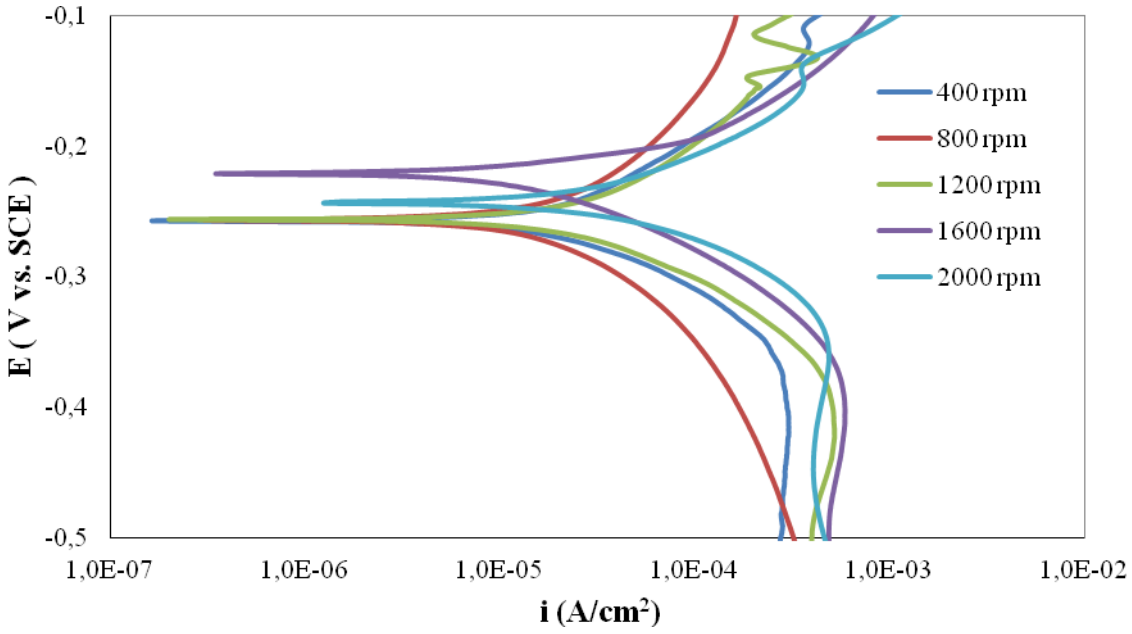

Figure 6. Polarization curves of the raw data for the alloy electrode NAV in aerated 0.1 M NaCl solution at 30^{o}C

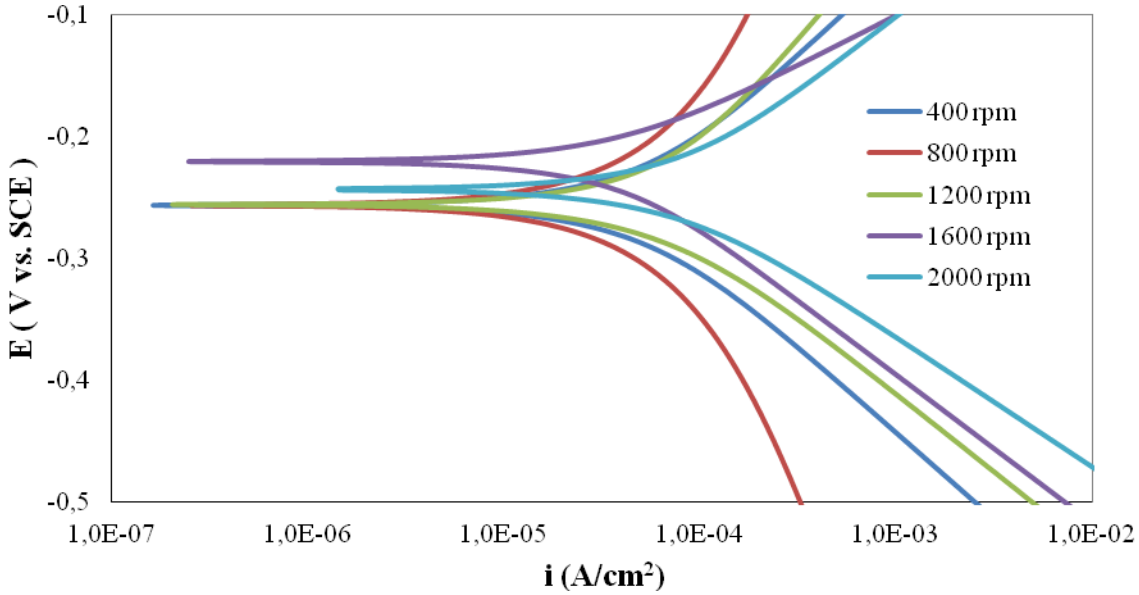

Figure 7. Curves Tafel polarization of adaptive methods toGamry software analysis Echem NAB alloy electrode in aerated 0.1 M NaCl solution at 30 ^{o}C.

In Figure 7, cathodic current density increases with the rotational speed of the electrodes that can be explained by the increase in the supply of oxygen to the surface of the alloy and the anodic current density does not have a clear trend because there is an error in the course of the corrosion experiments. In general, the anodic current density increases with the rotational speed of the electrode, which means dissolution of anodic alloy increases with the rotational speed of the electrode. Rotational speed of the electrode causes displacement of the corrosion potential, E_{corr} towards positive values, therefore, the anodic and cathodic current density increased. Through the polarization curves, it was found that when the electrode rotation speed increases, the polarization curves are shifted to higher corrosion current density.

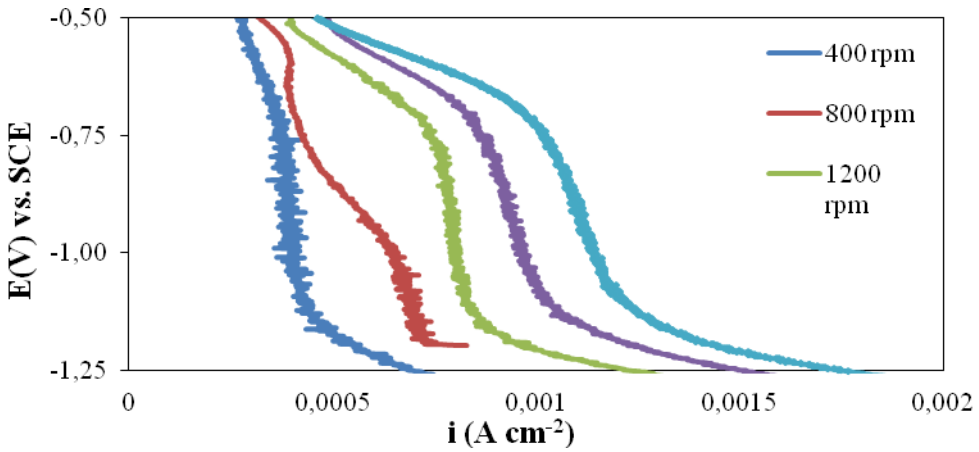

Figure 8. Cathodic polarization curves for NAB alloy in aerated solution of 0.1 M NaCl at different rotational speeds

Limiting current, iL can be obtained from polarization curves in the cathodic electrode with different rotational speeds in Figure 8. Cathodic reaction seems to be controlled by diffusion. From polarization curves obtained at different electrode rotation speed increases the limiting current observed with increasing rotational speed of the electrode, which may be caused by the increase in oxygen diffusivity even decrease concentration of oxygen mass transfer benefit.

At more negative potentials, there is mixed(charg e transfer and mass transport control) of the reaction rate androtat ion speed has an increasing effect as the potential is made more negative. Eventually, the potential is sufficiently negative for mass transport control of the reaction rate anda limiting current region is observed. At very negative potentials, the current again rises due to hydrogen evolution as a side reaction [31].

In aerated 0.1 M NaCl solution, involving the passage of anodic corrosion of copper ions from the surface of the alloy into the solution while the cathodic process involves the release of chloride ions. NAB alloy anodic dissolution is shown by the dissolution of most of the copper, Cu shown in equation 2. Electrochemical reaction to NAB alloys in aerated 0.1 M NaCl solution can be described by the following equation:

Anodic reaction: $Cu \rightarrow Cu^{2+} + 2e^{-}$ 2

$Cu + 2Cl^{-} \rightarrow CuCl_2^{-} + e^{-}$ 3

Cathodic reaction: $Cu + Cl^{-} \rightarrow CuCl + e^{-}$ 4

$Cl^{-} + 3H^{+} + 2e^{-} \rightarrow HCl + H_2O$ 5

$O_2 + 4H^{+} + 4e^{-} \rightarrow 2H_2O$ 6

In addition, the precipitation of copper chloride, CuCl on the surface of the alloy occurs because it has a low degree of solubility. Merurut to equation 3, this compound is stable in an inert atmosphere while in normal conditions as the absorption machine. Thus, after the formation of CuCl, copper anodic dissolution appear to be governed by $CuCl_2$ complex mass-transport from the surface into the solution through a layer of an alloy of CuCl. However, CuCl layer is characterized as weak and total precipitation of CuCl on the surface of the alloy is small because the flow of fluid out of the surface of the alloy layer of protection will be reduced and the corrosion rate increases with the rotational speed of the electrode. In addition, the cathodic reaction can also produce hydrogen chloride and water in small quantities.

Parameter values are available from potentiodynamic polarization measurement using Tafel fit routine calculations found in Gamry Echem. Analyst software such as corrosion current density, icorr, corrosion potential, Ecorr, Tafel coefficient of the anode, βa, cathodic Tafel coefficient, βc, the limiting current, iL and the corrosion rate with different electrode rotation speed at a temperature of 30^{o}C has been shown in Table 2 Linear velocity at the outer surface of the rotating cylinder electrode is calculated using the following equation

$$U = \omega\, r = \frac{\pi\ d\ F}{60} \qquad 7$$

Where, U = linear velocity in units of cm / s
ω = angular rotation rate in units of rad / s
F = angular rotation rate in rpm unit
d = diameter of rotating cylinder electrode in units of cm
In addition, the equation for the Reynolds number is shown as follows,

$$Re = \frac{U\ d\ \rho}{\mu} \qquad 8$$

Where, U = linear velocity in units of cm / s,
d = diameter of rotating cylinder electrode in units of cm.
ρ = density of the solution in g/cm3 units
μ = absolute viscosity of the solution in g / cm.s

In general, the Reynolds number for rotating cylinder electrode more than 200, the flow is turbulent flow. The corrosion rate can be calculated using the following equation in millimeters per year

$$\text{corrosion rate} = \frac{K \times i_{corr} \times \text{equivalent weight}}{\text{ketumpa tons}} \qquad 9$$

Where, K is a constant that defines the worth 3272 unit rate of corrosion is the corrosion current density, icorr in A cm^{-2} and the density in g cm^{-3}.

Refers to data that has been collected, the value of the corrosion potential, Ecorr shifted towards more positive while the value of the corrosion current density, icorr increases with the rotational speed of the NAB alloy electrode corrosion rate will increase.

Table 2. Data polarization potentiodynamic for NAB alloy in 0.1 M NaCl for different electrode rotation speed

speed rotation (rpm)	velocity linear,U (cm/s)	Reynold number (Re)	βa (V/dec)	βc (V/dec)	icorr (μA/cm2)	Ecorr (mV)	iL (mV)	The corrosion rate (mm/y)
400	25.13	7250.08	0.1387	0.1234	42.6	-256	-832.30	1.08
800	50.27	14500.17	0.5138	0.4811	56.3	-256	-846.75	1.42
1200	75.40	21750.25	0.1900	0.1282	61.5	-255	-816.45	1.56
1600	100.53	29000.34	0.0831	0.1214	69.8	-220	-817.35	1.77
2000	125.66	36250.42	0.1244	0.1065	72.5	-242	-817.80	1.84

Several workers [32–34] previously studied the polarization behavior of Cu in chloride solutions and showed that the Tafel region is not activation-controlled but a mass transport-kinetics process, whereby dissolution is controlled by the rate of diffusion of $CuCl_2$ species from the electrode surface across a diffusion layer whose concentration gradient is determined by the electrode potential. Mathematical analysis of such behavior showed that the apparent Tafel slope should be 59 mV/decade at room temperature, consistent with experimental data. Dhar [35] found the average anodic Tafel slopes of 70Cu–30Ni to be 60 mV/decade in 0.5 M NaCl, in good agreement with that of Cu. As E was further increased, the anodic Cu curve produced a small peak consistent with formation of a CuCl film [32,33] at a potential of __0.092VSCE. Beyond the peak, limiting-current behavior was obtained where the rate of anodic reaction was controlled by the formation and dissolution of a CuCl film [36].

4. CONCLUSION

Corrosion behavior of NAB alloy was studied under different flow speed. It was found that the corrosion rate increased with flow.

References

1. A. Tuthill, *Mater. Perform.*, 26 (1987) 12.
2. P. T., Gilbert, *J. Appl. Chem.*, 3 (1953) 174
3. V. P. K., Kochergin, M. F. Prostkov, and T. A., Nimvitskaya, *Konserv. Ovoshchesushil. Prom.*, 14 (1959) 22
4. V. E. Carter, and H. S., Campbell, *J. Inst. Met.*, 89 (1960) 472
5. V. E. Carter, and H. S., Campbell, *Br. Corros*. J., 4 (1969)15
6. R. J. McKay, and R., Worthington, Corrosion Resistance of Melals and Alloys, A.C.S. Monograph Series (1936)
7. S. C., Britton, The Corrosion Resistance of Tin and Tin Alloys, Tin Research Institute, Perivale, Middlesex (1951)
8. S. J., Harris, P. D. Green, and R. C., Cobb, Thermally Sprayed Al-Zn-In-Sn Alloys in 3rd Int. Conf. on Advances in Surface Engineering for Corrosion and Wear Resistance, Newcastle-upon-Tyne (1992) 1-10
9. R. J. Schmitt, and J. H., Rigo, *Materials Protection*, 5 (1966) 46-52
10. F. L. LaQue and H. R. Copson , editors, Corrosion Resistance of Metals and Alloys , Reinhold , New York (1963) 334 .
11. G. Wood and D. Melford , *J. Iron Steel Inst*. 198 (1961) 142.
12. ASTM B76 - 90, Standard Test Method for Accelerated Life of Nickel – Chromium and Nickel – Chromium – Iron Alloys for Electrical Heating , ASTM , West Conshohocken, PA (2007) .
13. A. Brasunas and H. H. Uhlig , ASTM Bulletin , ASTM , Philadelphia , 182 (1952) 71 .
14. Protection of Iron and Steel against Corrosion and Oxidation at Elevated Temperatures', Sprayed *Metal Coatings*, BS 2569: Part 2 (1965)
15. N. Birks , G. H. Meier , and F. S. Pettit , Introduction to the High Temperature Oxidation of Metals , 2nd edition, Cambridge University Press , Cambridge, U.K. , (2006) .
16. P. Kofstad , High - Temperature Oxidation of Metals , Wiley , New York , (1966) .
17. W. Robertson , *Trans. Am. Inst. Min. Metall. Eng.* 166 (1946) 216

18. U. Evans, The Corrosion and Oxidation of Metals , Arnold, London, (1960) 674.
19. B. Cox , Oxidation of zirconium and its alloys , Advances in Corrosion Science and Technology M. Fontana and R. Staehle , editors, Plenum Press , New York , 5 (1976) 173 .
20. F. Hasan, J. Iqbal and N. Ridley, *Materials Science Technology,* 1 (1985) 312.
21. F. Hasan, A. Jahanafrooz, G. W. Lorimer and N. Ridley, *Metallurgical Transactions A,* 13A (1982) 1337
22. ASTM, Standard terminology relating to corrosion and corrosion testing. Annual book of ASTM standards. 03 (2001) 02, ASTM, Philadelphia, Pa, USA.
23. T.E. Wright, H.P. Corrosion, 10 (1954) 195–198.
24. E.W. Jakson, *Chemical & Process Engineering*, 38 (1957) 391–393.
25. F.C. Porter, S.E. Hadden, *Journal of Applied Chemicals*, 3 (1953) 385–409.
26. A.M. Alfantazi, T.M. Ahmed, D. Tromans, *Materials and Design* 30 (2009) 2425.
27. J. R. Scully and R. G. Kelly , *Corrosion: Fundamentals, Testing, and Protection , ASM International , Materials Park, OH* , 13 (2003) 73 .
28. A. Yurt, S. Ulutas, H. Dal, *Surf. Sci.* 253 (2006) 919.
29. *G. Blustein, J. Rodriguez, R. Romanogli, C.F. Zinola, Corros. Sci. 47 (2005) 369.*
30. *R. Rosliza, H.B. Senin, W.B. Wan Nik, Colloid Surf. A 312 (2008) 185.*
31. *F.C. Walsh, A First Course in Electrochemical Engineering, The Electrochemical Consultancy, Romsey,* (1993).
32. *R. Rosliza, W.B. Wan Nik, H.B. Senin, Mater. Chem. Phys.* 107 (2008) 281.
33. AL, Bacarella, JC. Griesss . *J Electrochem Soc*, 120 (1973) 459.
34. D, Tromans, JC. Silva, *Corrosion*, 53 (1997) 171.
35. D, Tromans , R. Sun , *J Electrochem Soc*, 138 (1991) 3235.
36. P, Dhar. *Corrosion* 41 (1985) 193.